International Journal of Environmental Sciences
ISSN: 2229-7359
Vol. 11 No. 16s,2025
https://theaspd.com/index.php

Function-Based Comparison between *Proteus mirabilis* and *Bacillus paramycoides* by Rapid Annotation using Subsystem Technology

Sugitha S, Abirami G*
Department of Biotechnology, School of Life Sciences, Vels Institute of Science Technology and Advanced Studies, Pallavaram, Chennai, Tamil Nadu, India
*Corresponding author: Abirami G; Email Id: drabirami.cas@gmail.com

Abstract*; This study presents a comprehensive comparative analysis of Proteus mirabilis and Bacillus paramycoides through morphological, physiological, metabolic, and genomic assessments using data derived from BacDive, BV-BRC, SWISS-MODEL, RAST, SOPMA, and KEGG KAAS. Proteus mirabilis, a Gram-negative, motile bacterium, exhibits specialized features, thermal adaptability, and limited carbon source utilization. It shows robust enzymatic activities and significant antibiotic resistance, particularly to beta-lactam antibiotics, supported by genomic evidence of beta-lactam biosynthesis and resistance pathways. In contrast, Bacillus paramycoides, a Gram-positive facultative anaerobe with inconsistent motility and spore-forming traits, displays broader metabolic versatility, enhanced environmental adaptability, and a rich enzymatic profile suitable for biotechnological applications. Structural modeling of Metallothionein proteins revealed that B. paramycoides possesses a structurally superior model with higher sequence identity and better validation scores than P. mirabilis, despite both exhibiting alpha-helical dominance. Metallothionein, a heavy metal-binding protein found in both organisms, suggests potential utility in heavy metal bioremediation strategies. These findings highlight the contrasting ecological roles and biotechnological potentials of both organisms, with B. paramycoides offering greater promise for environmental resilience and metal detoxification applications.*

Keywords*: Proteus mirabilis; Bacillus paramycoides; BacDive; SWISS-MODEL; Metallothionein; and Beta-lactam*

INTRODUCTION

Environmental pollution, especially due to industrialization and urbanization, has emerged as a formidable global challenge. The escalation of pollutants, ranging from heavy metals, hydrocarbons, dyes, pharmaceuticals, to other xenobiotics, has led to the contamination of soil, water, and air, jeopardizing ecosystems and human health. Conventional physical and chemical remediation methods, although effective in certain contexts, often incur high costs, generate secondary pollution, and may not be sustainable in the long term. Consequently, bioremediation has gained significant attention as a cost-effective, eco-friendly, and sustainable alternative for the detoxification and restoration of polluted environments[1], [2], [3].Bioremediation harnesses the innate degradative capabilities of microorganisms to transform or detoxify hazardous compounds into less harmful or inert products. Microorganisms such as bacteria, fungi, and algae possess diverse enzymatic systems capable of degrading complex organic and inorganic pollutants[4], [5], [6]. The success of bioremediation depends heavily on understanding the metabolic pathways, enzymatic mechanisms, and environmental adaptations of these microorganisms. Among various microbial candidates, bacteria are particularly advantageous due to their rapid growth, genetic manipulability, and metabolic diversity[7], [8], [9].A multitude of bacterial genera, including *Proteus*, *Bacillus*, *Pseudomonas*, *Acinetobacter*, and *Rhodococcus*, have been extensively studied for their pollutant-degrading capabilities[10], [11]. For instance, *Proteus mirabilis* is a Gram-negative bacterium traditionally known for its pathogenicity and role in urinary tract infections, but recent studies have revealed its potential in bioremediation processes, including degradation of organic matter and heavy metals under specific conditions. Its enzymatic repertoire offers promising avenues for pollutant breakdown, making it a subject of interest in environmental biotechnology[12], [13], [14], [15].On the other hand, members of the genus *Bacillus*, such as *Bacillus paramycoides*, are Gram-positive, spore-forming bacteria renowned not only for their robustness and ability to survive harsh conditions but also for their diverse metabolic pathways. *Bacillus* species are extensively used in bioremediation owing to their capacity to produce a plethora of extracellular enzymes—including proteases, lipases, and oxidoreductases—that facilitate the degradation of various pollutants[16], [17], [18]. *Bacillus paramycoides*, a relatively recent

addition to this genus, has shown potential in breaking down complex organic compounds, making it an attractive candidate for biotechnological applications[19], [20].Deciphering the genetic and metabolic potential of these microorganisms is essential to understanding and optimizing their bioremediation capabilities. Traditional genomic analyses, while informative, can be time-consuming and may not efficiently highlight functional gene clusters responsible for pollutant degradation. Advances in bioinformatics, such as Rapid Annotation using Subsystem Technology (RAST), have revolutionized microbial genome analysis by providing quick, automated, and comprehensive annotations[21], [22], [23]. RAST assigns genomic features to functional subsystems, enabling researchers to identify genes involved in specific metabolic pathways, resistance mechanisms, and enzymatic activities related to bioremediation[24], [25]. Applying such high-throughput annotation methods allows for a function-based comparison of *Proteus mirabilis* and *Bacillus paramycoides*, shedding light on their respective genetic determinants for pollutant degradation. This comparative analysis not only enhances our understanding of their biodegradation potential but also helps in identifying genetic markers for strain improvement, enzyme production, and process optimization.Despite the recognized bioremediation potential of *Proteus mirabilis* and *Bacillus* species, there remains a knowledge gap regarding their comparative functionalities at the genomic and metabolic levels. Most previous studies have focused on isolated degradation assays or partial genomic analyses, limiting comprehensive insights into their full bioremediation potential. This study aims to bridge this gap by performing a detailed, function-based comparison of *Proteus mirabilis* and *Bacillus paramycoides* genomes using RAST annotation and other bioinformatic tools.

MATERIALS AND METHODS

Retrieval of Physiological and Metabolic Data of *Proteus mirabilis* and *Bacillus paramycoides* from BacDive and BV-BRC.Physiological and metabolic data of *Proteus mirabilis* and *Bacillus paramycoides* were retrieved from the BacDive (The Bacterial Diversity Metadatabase) (https://bacdive.dsmz.de/) and BV-BRC (Bacterial and Viral Bioinformatics Resource Center) (https://www.bv-brc.org/) databases[26], [27], [28]. Advanced search tools were used to locate strain-specific entries using scientific names and taxonomic identifiers. Data fields including temperature range, pH tolerance, oxygen requirements, enzyme activities, and substrate utilization were selected. Relevant records were downloaded or manually extracted for comparison and analysis. The retrieved data were compiled and used to support experimental findings on bacterial growth and bioremediation potential[29], [30].Analysis of Subsystem Category Distribution Using RAST for Proteus mirabilis and Bacillus paramycoides.The annotated genome sequences of *Proteus mirabilis* and *Bacillus paramycoides* were uploaded to the RAST (Rapid Annotation using Subsystem Technology) (https://rast.nmpdr.org/seedviewer.cgi) server for functional analysis. Genomes were processed using default parameters with the RASTtk pipeline to ensure high-quality, consistent annotations. Upon completion, subsystem category distribution statistics were retrieved, detailing the number of genes associated with various functional categories. Key subsystems included metabolism of amino acids, carbohydrates, proteins, cofactors, and stress response pathways. The output was exported in tabular and graphical formats for comparative interpretation[24], [25].

Pathway Mapping and Analysis of Beta-Lactam Resistance in *Proteus mirabilis* and *Bacillus paramycoides* Using KEGG KAAS.The annotated genomes of *Proteus mirabilis* and *Bacillus paramycoides* were submitted to the KEGG Automatic Annotation Server (KAAS) (https://www.genome.jp/tools/kaas/) for pathway mapping. KEGG Orthology (KO) assignments were generated using the bidirectional best hit (BBH) method. The beta-lactam resistance pathway (ko01501) was specifically analyzed in both organisms. Enzymes and resistance genes involved in antibiotic inactivation, target modification, and efflux mechanisms were identified. Comparative analysis was performed to determine the presence and variation of resistance determinants between the two species[31], [32], [33].Secondary Structure Prediction of Proteins from *Proteus mirabilis* and *Bacillus paramycoides* Using SOPMA, Protein sequences of interest from *Proteus mirabilis* and *Bacillus paramycoides* were retrieved from the RCSB Protein Data Bank (PDB) by searching with organism names and relevant protein identifiers. The sequences were downloaded in FASTA format for further analysis. Selected proteins were chosen based on their roles in resistance or metabolic pathways relevant to the study. The FASTA sequences were then submitted to the SOPMA (Self-Optimized Prediction Method with Alignment) server for secondary structure prediction.

SOPMA was run with default parameters, including a window width of 17 and a similarity threshold of 8[34], [35], [36]. The output provided percentage distributions of alpha helices, beta sheets, turns, and random coils. The results were interpreted to understand the structural characteristics of proteins involved in functional and adaptive responses.

Homology Modeling and Structural Validation of Proteins from *Proteus mirabilis* and *Bacillus paramycoides* Using SWISS-MODEL

The tertiary structures of selected proteins from *Proteus mirabilis* and *Bacillus paramycoides* were predicted using the SWISS-MODEL homology modeling server (https://swissmodel.expasy.org/). Protein sequences in FASTA format were submitted to the server, which automatically identified suitable templates based on sequence similarity. The best template for each protein was selected based on GMQE and QMEAN scores to ensure structural accuracy. 3D models were generated and visually analyzed for structural integrity and functional relevance. The predicted models were further evaluated using validation tools such as the Ramachandran plot and ProSA-web[37], [38], [39], [40].

RESULTS AND DISCUSSION

Physiological and Metabolic Data of *Proteus mirabilis* and *Bacillus paramycoides* from BacDive and BV-BRC

Morphological and Colony Characteristics

Proteus mirabilis is a Gram-negative, rod-shaped, motile bacterium with strong confidence from genome prediction (98.985% for Gram-negative and 73.915% for motility). Its motility is further supported by observed growth patterns. In contrast, Bacillus paramycoides is Gram-positive, rod-shaped, with a cell size of 1.8–2.2 µm in length and 0.8–1.2 µm in width. However, motility status is conflicting for Bacillus paramycoides, with both positive and negative reports, though genome predictions suggest it is flagellated (83% confidence). Its colonies are circular and moderately sized (2–3 mm), grown on LB agar (refer to Table 1 and 2).

Culture and Growth Conditions

Both organisms have broad growth temperature ranges, but *Proteus mirabilis* shows wider thermal tolerance, growing from 5°C to 41°C, with optima at 30°C and 37°C, which suits environmental and clinical settings. *Bacillus paramycoides* grows between 15°C and 39°C, optimally at 28–30°C, and tolerates a NaCl range of 0–5% (optimum at 0.5%), indicating moderate halotolerance. In terms of pH, *Bacillus* tolerates pH 5.0–9.0 with an optimum at pH 7, whereas such pH tolerance wasn't explicitly listed for *Proteus mirabilis* (refer to Table 1 and 2).

Physiological Traits and Oxygen Tolerance

Bacillus paramycoides is a facultative anaerobe, non-spore-forming (experimentally), but genome prediction contradicts this slightly with a 69.5% likelihood of spore formation. *Proteus mirabilis* is non-aerobic and non-anaerobic based on genome prediction, suggesting it might rely on microaerophilic or alternative respiration modes not well-captured in the database, which may require experimental verification. Both organisms are non-thermophilic.

Metabolism and Biochemical Traits

Proteus mirabilis exhibits positive methyl red test and negative Voges-Proskauer test, consistent with mixed-acid fermentation. It produces hydrogen sulfide and utilizes a limited set of carbon sources such as glucose, D-glucose, D-mannitol, and citrate, while being negative for amygdalin, arginine, and L-arabinose. *Bacillus paramycoides*, on the other hand, is positive for acetoin and Voges-Proskauer, but does not produce hydrogen sulfide or indole, indicating different metabolic end products. It uses a broader range of carbon sources including amygdalin, arabinose, arbutin, casein, cellobiose, and citrate, showing metabolic versatility. It does not utilize compounds like 2-/5-dehydro-D-gluconate or D-arabinose.

Enzymatic Profiles

Proteus mirabilis has a wide array of enzyme activities, including acid and alkaline phosphatases, alcohol dehydrogenase, and alpha-glucosidase, indicating strong metabolic capacity. *Bacillus paramycoides* tests positive for catalase, cytochrome oxidase, gelatinase, and urease, but negative for arginine dihydrolase and beta-galactosidase, suggesting differences in nitrogen and carbohydrate processing.

Antibiotic Susceptibility

Only *Proteus mirabilis* data includes antibiotic susceptibility. It shows high sensitivity to ampicillin, ticarcillin, cefotaxime, and imipenem, while being resistant to oxacillin (0 mm inhibition zone). This profile is relevant in clinical settings, especially in urinary tract infections where this species is commonly involved.

Genome-Based Predictions

From genome-based predictions, *Proteus mirabilis* is confirmed to be Gram-negative, motile, and non-spore-forming, with moderate to high confidence levels. Interestingly, it is predicted as non-aerobic and non-anaerobic, which may point to facultative or alternative respiration capabilities. *Bacillus paramycoides*, in contrast, is predicted to be Gram-positive, flagellated, and spore-forming, although lab results indicate it may not actually form spores. This discrepancy underlines the importance of corroborating genome-based predictions with phenotypic observations.

Proteus mirabilis displays characteristics of a robust Gram-negative pathogen with defined metabolic and antibiotic resistance profiles, well-suited to clinical environments. *Bacillus paramycoides*, meanwhile, shows broader metabolic versatility, facultative anaerobic growth, and a Gram-positive profile, making it potentially useful for environmental or industrial applications. Their enzymatic and physiological differences suggest distinct ecological niches and applications, with *Proteus* being more pathogenic and *Bacillus* possibly more biotechnologically relevant.

Table 1: Morphological, Physiological, and Biochemical Features of *Proteus mirabilis*

Category	Attributes	Details
Morphology	Gram stain	Negative (Confidence: 98.985%)
	Cell shape	Rod-shaped
	Motility	Yes
Culture Conditions	Culture medium	CIP Medium 72
	Growth temperature range	5–41 °C
	Optimal temperatures	30 °C, 37 °C
Antibiotic Susceptibility	Penicillin G	20–26 mm inhibition zone
	Oxacillin	0 mm (Resistant)
	Ampicillin	28–30 mm
	Ticarcillin	32–38 mm
	Cefotaxime	44 mm
	Imipenem	32–34 mm
Metabolite Utilization	Fermentation/assimilation	Positive for citrate, glucose, D-glucose, D-mannitol
	Negative for	Amygdalin, Arginine, L-arabinose
Metabolite Production	Hydrogen sulfide	Yes
	Indole, Acetoin	No
Physiological Tests	Methyl red test	Positive
	Voges-Proskauer test	Negative
Enzyme Activities	Positive enzymes	Acid phosphatase, Alcohol dehydrogenase, Alkaline phosphatase, Alpha-glucosidase, etc.
Genome-Based Predictions	Aerobic	No (Confidence: 74.23%)
	Anaerobic	No (Confidence: 91.236%)
	Motile	Yes (Confidence: 73.915%)
	Spore-forming, Thermophilic	No

Table 2: Morphological, Physiological, and Biochemical Features of *Proteus mirabilis*

Category	Attributes	Details
Morphology	Gram stain	Positive
	Cell shape	Rod-shaped
	Cell length	1.8–2.2 µm
	Cell width	0.8–1.2 µm
	Motility	Conflicting (both "no" and "yes" reported)
Colony Features	Colony size	2–3 mm
	Colony shape	Circular
	Incubation period	2 days
	Cultivation medium	Luria-Bertani agar
Culture Conditions	Culture media	LB (Luria-Bertani), Trypticase soy agar, CIP Medium 72
	Temperature (growth range)	15–39°C
	Temperature (optimum)	28–30°C
	pH (growth range)	5.0–9.0
	pH (optimum)	7
Physiology	Oxygen tolerance	Facultative anaerobe
	Spore formation	No
	Salt tolerance (NaCl)	Growth: 0–5%, Optimum: 0.5%
Metabolism	Acetoin production	Yes
	Hydrogen sulfide/Indole	No
	Voges-Proskauer test	Positive
Enzymatic Activity	Catalase, cytochrome oxidase, etc.	Positive for catalase, cytochrome oxidase, gelatinase, urease
	Other enzymes	Negative for arginine dihydrolase, beta-galactosidase, etc.
Carbon Source Utilization	Amygdalin, arabinose, arbutin, casein, cellobiose, citrate	Utilized
	2-/5-dehydro-D-gluconate, D-arabinose	Not utilized
Genome-based Predictions	Gram-positive	Yes (76.5% confidence)
	Spore-forming	Yes (69.5% confidence)
	Flagellated	Yes (83.0% confidence)
	Anaerobic	No (94.3% confidence)
	Aerobic	No (57.5% confidence)
	Thermophilic	No (94.8% confidence)

Analysis of Subsystem Category Distribution Using RAST for *Proteus mirabilis* and *Bacillus paramycoides*

The RAST-based subsystem category distribution analysis reveals notable differences between *Proteus mirabilis* and *Bacillus paramycoides*, reflecting their ecological roles and metabolic potentials. *Proteus mirabilis* demonstrates a higher subsystem coverage (53%) compared to *Bacillus paramycoides* (38%), suggesting that a larger proportion of its genes are associated with well-characterized biological functions. This higher annotation confidence in *P. mirabilis* aligns with its role as a motile opportunistic pathogen, supported by the elevated number of features related to motility and chemotaxis (57), stress response (183), membrane transport (192), and cell wall and capsule synthesis (180) (Fig. 1). These subsystems are crucial for adaptation, host interaction, and survival under challenging conditions.

In contrast, *Bacillus paramycoides* shows a stronger emphasis on core metabolic functions, particularly with significantly higher counts in amino acids and derivatives (497), carbohydrates (425), and protein metabolism (269). These features are indicative of a metabolically versatile bacterium, likely well-suited

for survival and competition in diverse environmental niches. Additionally, *B. paramycoides* exhibits more genes associated with virulence, disease, and defense (111), as well as phosphorus and iron acquisition, which may enhance its ecological adaptability (refer to Table 3 and Fig. 2). Despite its lower subsystem coverage, the presence of a wide array of functional genes hints at a potentially broader but less annotated genetic repertoire.

Overall, the comparison illustrates that *Proteus mirabilis* is more specialized in traits linked to pathogenicity and environmental stress tolerance, whereas *Bacillus paramycoides* possesses a richer profile of metabolic capabilities, possibly reflecting its saprophytic lifestyle and environmental resilience.

Table 3: Subsystem Category Distribution of *Proteus mirabilis* and *Bacillus paramycoides*

Subsystem	P. mirabilis	B. paramycoides	Observation
Amino Acids and Derivatives	367	497	More in *B. paramycoides*
Carbohydrates	350	425	Higher in *B. paramycoides*
Cofactors, Vitamins, Pigments	277	295	Similar, but more in *B. paramycoides*
Protein Metabolism	201	269	Higher in *B. paramycoides*
RNA Metabolism	213	214	Nearly equal
DNA Metabolism	139	134	Nearly equal
Membrane Transport	192	100	Significantly higher in *P. mirabilis*
Cell Wall and Capsule	180	140	More in *P. mirabilis*
Stress Response	183	107	Higher in *P. mirabilis*
Virulence, Disease and Defense	76	111	Higher in *B. paramycoides*
Secondary Metabolism	5	10	Slightly higher in *B. paramycoides*
Phages, Prophages, Transposable Elements	6	4	Slightly higher in *P. mirabilis*
Motility and Chemotaxis	57	7	Significantly higher in *P. mirabilis*
Photosynthesis	0	0	Absent in both

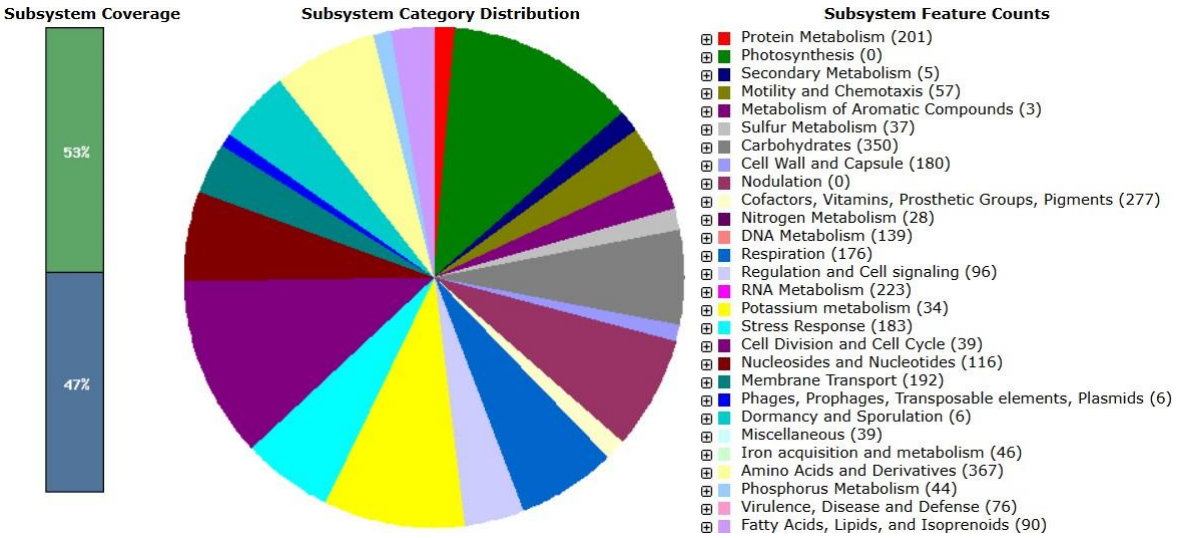

Fig. 1 Subsystem Category Distribution of *Proteus mirabilis*

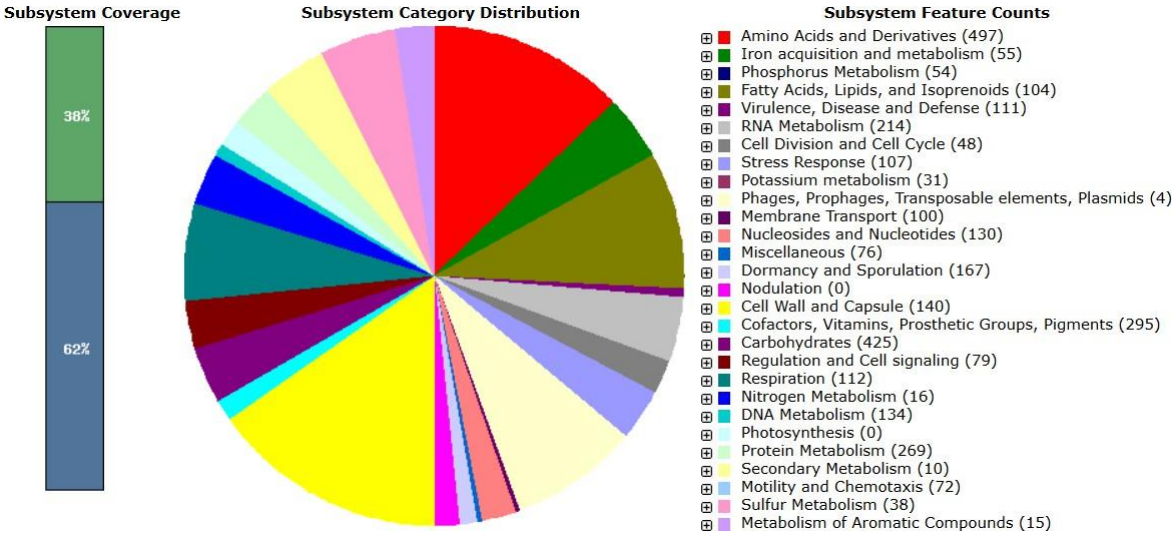

Fig. 2 Subsystem Category Distribution of *Bacillus paramycoides*

Pathway Mapping and Analysis of Beta-Lactam Resistance in *Proteus mirabilis* and *Bacillus paramycoides* Using KEGG KAAS

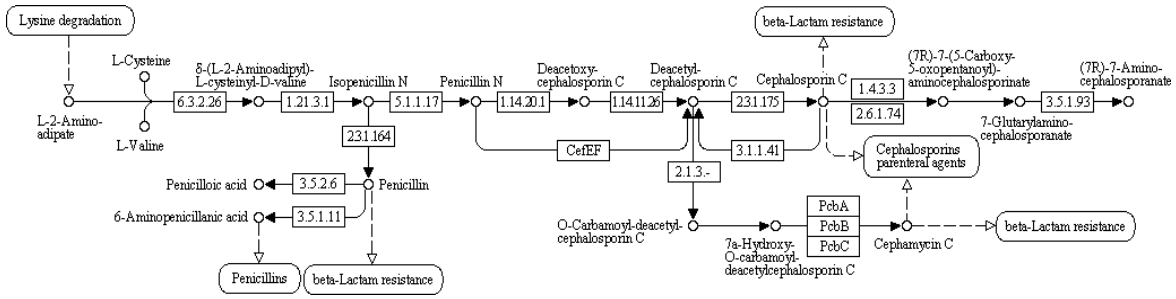

Fig. 3 KEGG pathway of Beta-Lactam Resistance in *Proteus mirabilis* and *Bacillus paramycoides*

The KEGG pathway map illustrates the biosynthesis of beta-lactam antibiotics and the associated resistance mechanisms, highlighting key steps in the formation and modification of penicillin and cephalosporin compounds. The pathway begins with lysine degradation, where L-2-aminoadipate—derived from lysine—is converted through a series of enzymatic reactions involving L-cysteine and L-valine. These precursors, under the action of enzymes like 6.3.2.26 and 1.21.3.1, ultimately lead to the synthesis of isopenicillin N, which is the central intermediate for the production of both penicillins and cephalosporins.

From isopenicillin N, the pathway diverges into two branches. The penicillin branch converts isopenicillin N into penicillin N, which is then processed into 6-aminopenicillanic acid and penicilloic acid through the actions of enzymes 3.5.2.6 and 3.5.1.11. These are essential forms of penicillins used in antibiotic formulations. In parallel, the cephalosporin branch involves the transformation of penicillin N into deacetoxycephalosporin C and further into cephalosporin C via enzymes such as 1.14.20.1, 1.14.11.26, and 2.1.3(Fig. 3). Cephalosporin C can be further modified into cephamycin C and other derivatives, aided by enzymes like PcbA, PcbB, PcbC, and CefEF.

An important aspect of this pathway is the integration of beta-lactam resistance mechanisms. Resistance is conferred primarily through the activity of beta-lactamase enzymes, which cleave the beta-lactam ring, rendering the antibiotic ineffective. Additionally, modifications in antibiotic targets and efflux mechanisms further enhance resistance. These resistance elements are shown interacting within the pathway, indicating that bacteria possessing this pathway can not only produce but also resist beta-lactam antibiotics.

In the case of *Proteus mirabilis* and *Bacillus paramycoides*, both organisms share this complete beta-lactam biosynthesis and resistance pathway. This suggests that they possess the genetic and enzymatic tools to engage in both the synthesis and detoxification of beta-lactam antibiotics. *Proteus mirabilis* is a well-known opportunistic pathogen frequently involved in urinary tract infections and is commonly resistant to beta-lactams via extended-spectrum beta-lactamases (ESBLs). *Bacillus paramycoides*, although more commonly found in environmental contexts, also displays similar genomic capabilities, raising concerns about its role in antimicrobial resistance dissemination.

In summary, the shared presence of the beta-lactam pathway in both organisms underscores their potential roles in the production and resistance to beta-lactam antibiotics. This highlights the broader ecological and clinical implications, especially regarding the spread of resistance traits in both pathogenic and non-pathogenic bacterial communities.

Secondary Structure Prediction of Protein Metallothionein from *Proteus mirabilis* and *Bacillus paramycoides* Using SOPMA

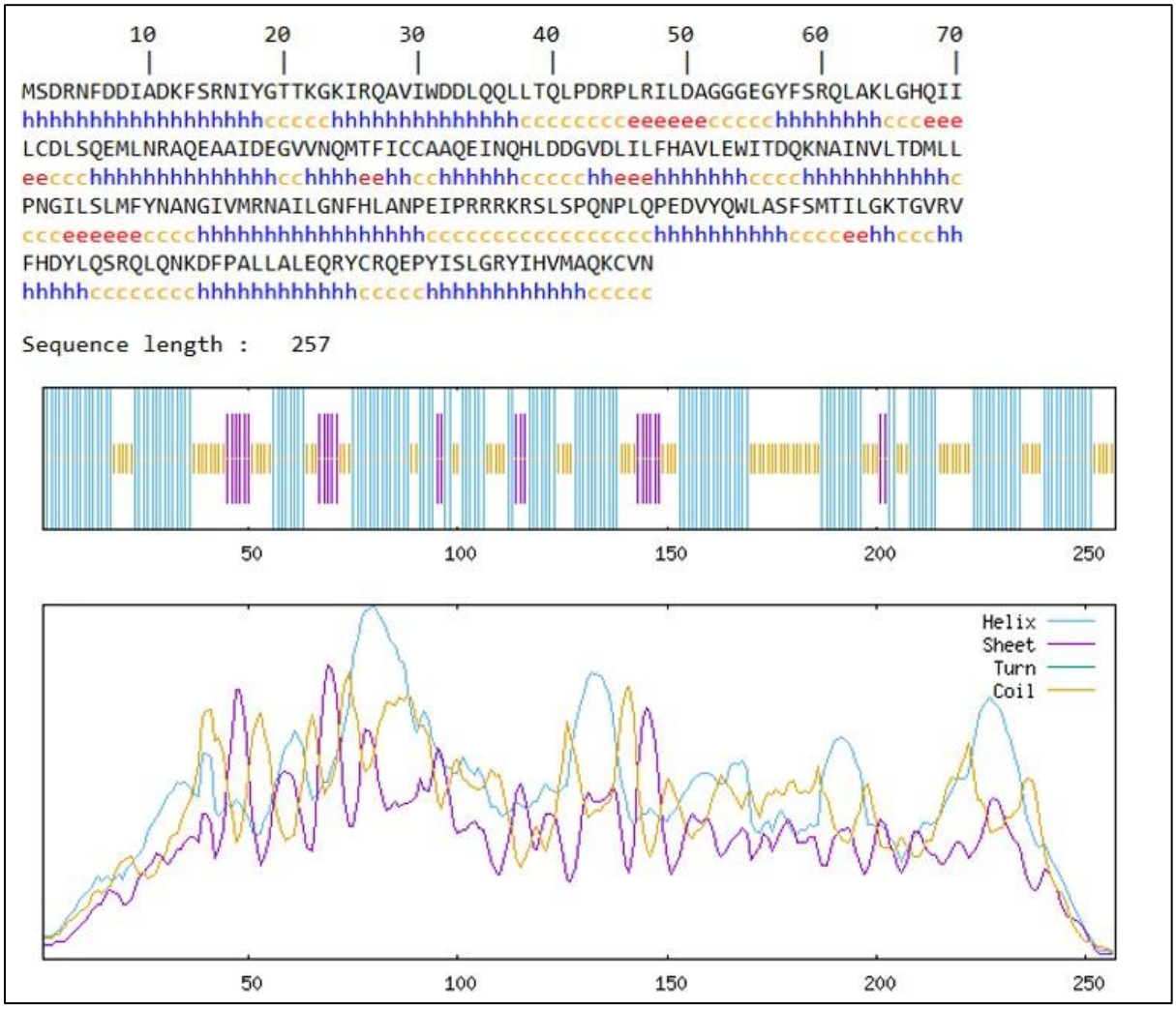

Fig. 4 Secondary Structure Prediction of Protein Metallothionein from *Proteus mirabilis*

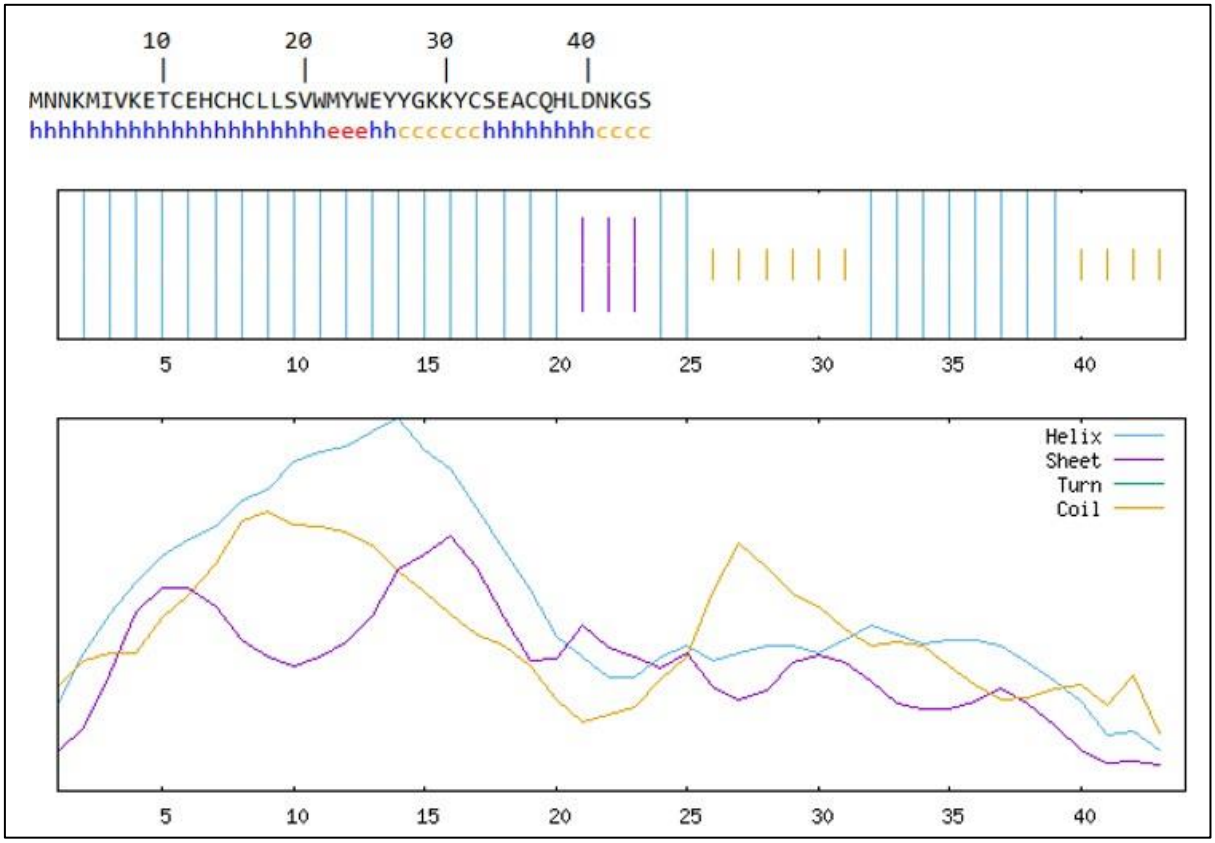

Fig. 5 Secondary Structure Prediction of Protein Metallothionein from *Bacillus paramycoides*

The secondary structure prediction of selected proteins from *Proteus mirabilis* and *Bacillus paramycoides* using the SOPMA tool reveals notable differences and similarities in their structural composition. Both proteins exhibit a predominant presence of alpha-helices, which is a common feature in proteins involved in functional activities such as enzymatic catalysis, molecular recognition, and resistance mechanisms. In *Proteus mirabilis*, the protein Metallothionein (GenBank: VEB84384.1) consists of 257 amino acids, with alpha helices making up approximately 56.81% of its structure (Fig. 4). This significant proportion of helices suggests a well-organized, stable protein conformation that may support functions like substrate binding or resistance to environmental stressors.

While, the protein Metallothionein from *Bacillus paramycoides* (GenBank: QDZ76690.1) displays an even higher alpha-helical content at 70.45%, indicating a more compact and structurally rigid protein. This high helicity may contribute to enhanced stability under environmental stress or during metabolic processes. However, the total length of this protein is shorter, and it features a lower percentage of random coils (22.73%) compared to the *Proteus mirabilis* protein, which has 33.85% random coil regions. Random coils represent flexible and disordered regions that often allow for dynamic interactions with other molecules, suggesting that the *Proteus* protein may have greater structural adaptability. The beta-sheet content, represented as extended strands, is low in both proteins—9.34% in *Proteus mirabilis* and 6.82% in *Bacillus paramycoides* (Fig. 5). This indicates that beta-sheet-driven stability is not a dominant feature in these proteins.

But in comparison, the results indicate that while both proteins are alpha-helix rich, the *Proteus mirabilis* protein possesses a more balanced distribution between helical and flexible coil regions, possibly providing it with greater functional versatility. In contrast, the *Bacillus paramycoides* protein is more rigid and helix-dense, which might reflect a more specialized or robust structural role. These structural differences could be linked to each organism's ecological niche or resistance capabilities.

Homology Modeling and Structural Validation of Protein Metallothionein from *Proteus mirabilis* and *Bacillus paramycoides* Using SWISS-MODEL

The homology modeling and structural validation of the Metallothionein proteins from *Proteus mirabilis* and *Bacillus paramycoides* using SWISS-MODEL provide comparative insights into the quality and

International Journal of Environmental Sciences
ISSN: 2229-7359
Vol. 11 No. 16s,2025
https://theaspd.com/index.php

reliability of the predicted three-dimensional structures. For *Proteus mirabilis*, the Metallothionein model yielded a GMQE score of 0.30 and a QMEANDisCo Global score of 0.52 ± 0.07, reflecting moderate confidence in the predicted structure. The sequence identity to the template was relatively low at 19.18%, which may compromise structural accuracy. Additionally, the MolProbity score of 2.70 and clash score of 6.99 suggest some stereochemical inconsistencies and minor steric clashes within the model (Fig. 6). Furthermore, 82.72% of the residues were located in the Ramachandran favored regions, indicating that a majority of the backbone conformations are geometrically acceptable, though the model still has scope for improvement (Fig. 7).

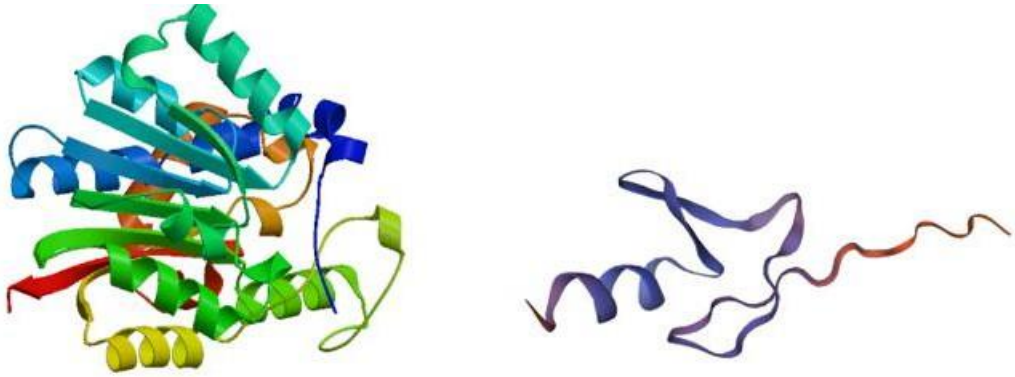

(A) (B)

Fig. 6 Homology Modeling of Protein Metallothionein from (A) *Proteus mirabilis* and (B)*Bacillus paramycoides*

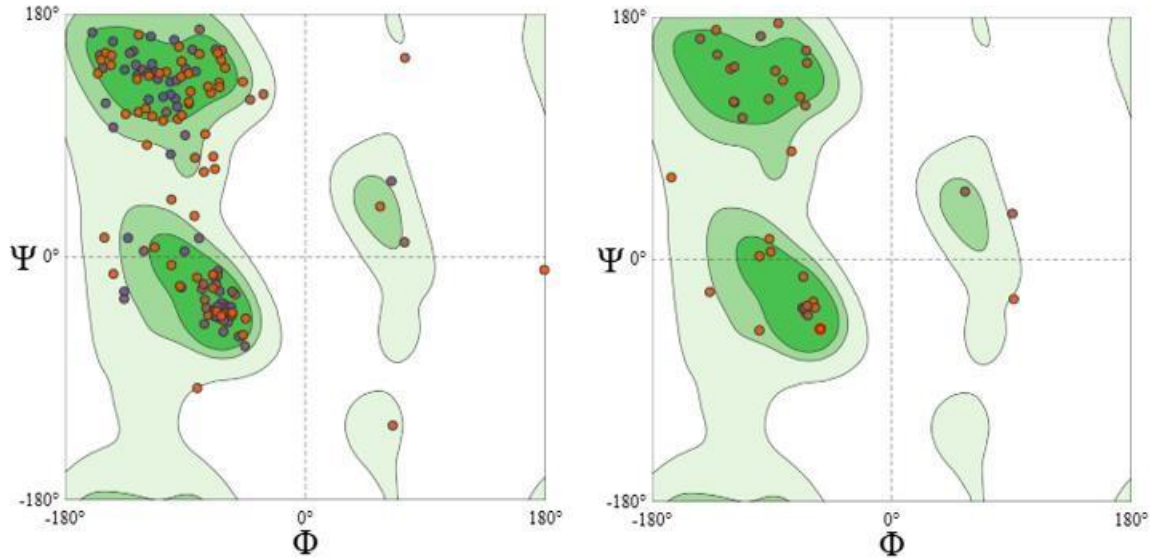

(A) (B)

Fig. 7 Ramachandran plot for Metallothionein (A) *Proteus mirabilis* (B) *Bacillus paramycoides*

Conversely, the Metallothionein protein model from *Bacillus paramycoides* shows overall better structural quality. It exhibited a higher GMQE score of 0.42 and a sequence identity of 33.33%, indicating a closer match to the template and hence a more reliable model. Despite a slightly lower QMEANDisCo Global score of 0.48 ± 0.12, the model's geometry was superior, supported by a MolProbity score of 2.49 and a clash score of 6.34, both of which reflect improved atomic interactions and structural refinement. Notably, 89.19% of residues were found in the Ramachandran favored regions, reinforcing the model's accuracy in terms of backbone dihedral angles.

CONCLUSION

The comparative investigation of *Proteus mirabilis* and *Bacillus paramycoides* reveals significant physiological, metabolic, and structural divergences that reflect their distinct ecological adaptations and potential applications. *P. mirabilis* demonstrates specialized antibiotic resistance mechanisms, limited substrate utilization, and robust enzymatic traits. The structural and secondary structure analyses of its Metallothionein protein support a moderately stable configuration with a balance of helices and coils, suitable for adaptive functionality. Conversely, *B. paramycoides* demonstrates greater metabolic flexibility, broader substrate utilization, and a higher-quality structural model for Metallothionein, making it better suited for environmental or industrial roles. The enriched core metabolic pathways and broader enzymatic spectrum in *B. paramycoides* reinforce its role as a saprophyte with biotechnological promise. Notably, Metallothionein proteins from both organisms exhibit properties suitable for binding heavy metals, highlighting their potential application in heavy metal bioremediation approaches. Additionally, the presence of beta-lactam biosynthesis and resistance pathways in both organisms underscores the importance of monitoring antimicrobial resistance in both environmental and non-clinical bacterial communities. Overall, this study emphasizes the importance of integrative genomic, structural, and phenotypic approaches in elucidating microbial roles and potentials.

Acknowledgements

We are grateful to Vels Institute of Science, Technology and Advanced Studies (VISTAS) for generously providing the facilities and space to conduct our research.

Data Availability

The data supporting the findings of this study are available from the corresponding author upon reasonable request.

Funding: The authors declare that no grants, funding, or other financial support were received for the research and publication of the manuscript.

Declarations

Conflict of interest: The authors declare no competing interest.

Consent for Publication: All authors agree to publish the following manuscript

REFERENCE

[1] A. Patel, R. Singhania, F. P. J. Albarico, A. Pandey, C. Chen, and C. Dong, "Organic wastes bioremediation and its changing prospects.," *Sci Total Environ*, p. 153889, 2022, doi: 10.1016/j.scitotenv.2022.153889.

[2] S. Bala *et al.*, "Recent Strategies for Bioremediation of Emerging Pollutants: A Review for a Green and Sustainable Environment," *Toxics*, vol. 10, p., 2022, doi: 10.3390/toxics10080484.

[3] P. Sar, S. Kundu, A. Ghosh, and B. Saha, "Natural surfactant mediated bioremediation approaches for contaminated soil," *RSC Adv*, vol. 13, pp. 30586–30605, 2023, doi: 10.1039/d3ra05062a.

[4] S. AbuQamar *et al.*, "Exploiting fungi in bioremediation for cleaning-up emerging pollutants in aquatic ecosystems.," *Mar Environ Res*, vol. 190, p. 106068, 2023, doi: 10.1016/j.marenvres.2023.106068.

[5] Dvořák, "Bioremediation 3.0: Engineering pollutant-removing bacteria in the times of systemic biology.," *Biotechnol Adv*, vol. 35 7, pp. 845–866, 2017, doi: 10.1016/j.biotechadv.2017.08.001.

[6] M. Narayanan, S. Ali, and M. El-Sheekh, "A comprehensive review on the potential of microbial enzymes in multipollutant bioremediation: Mechanisms, challenges, and future prospects.," *J Environ Manage*, vol. 334, p. 117532, 2023, doi: 10.1016/j.jenvman.2023.117532.

[7] D. Kour *et al.*, "Beneficial microbiomes for bioremediation of diverse contaminated environments for environmental sustainability: present status and future challenges," *Environmental Science and Pollution Research*, vol. 28, pp. 24917–24939, 2021, doi: 10.1007/s11356-021-13252-7.

[8] S. Bala *et al.*, "Recent Strategies for Bioremediation of Emerging Pollutants: A Review for a Green and Sustainable Environment," *Toxics*, vol. 10, p., 2022, doi: 10.3390/toxics10080484.

[9] A. Bhaskaralingam *et al.*, "Bioremediation of pharmaceuticals waste and pesticides using various microorganisms: A review," *Process Safety and Environmental Protection*, p., 2024, doi: 10.1016/j.psep.2024.12.050.

[10] K. Bhowmick *et al.*, "Potential microbes in bioremediation: A review," *Materials Today Sustainability*, p., 2024, doi: 10.1016/j.mtsust.2024.101032.

[11] X. Li, S. Wu, Y. Dong, H. Fan, Z. Bai, and X. Zhuang, "Engineering Microbial Consortia towards Bioremediation," *Water (Basel)*, p., 2021, doi: 10.3390/w13202928.

[12] R. Wasfi, S. Hamed, M. Amer, and L. Fahmy, "Proteus mirabilis Biofilm: Development and Therapeutic Strategies," *Front Cell Infect Microbiol*, vol. 10, p., 2020, doi: 10.3389/fcimb.2020.00414.

[13] R. Ganorkar, N. Jadeja, A. Shanware, and A. Ingle, "Characterisation of novel microbial strains Proteus mirabilis and Bordetella avium for heavy metal bioremediation and dye degradation," *Arch Microbiol*, vol. 204, p., 2022, doi: 10.1007/s00203-022-02873-2.

[14] C. Ke *et al.*, "Biotreatment of oil sludge containing hydrocarbons by Proteus mirabilis SB," *Environ Technol Innov*, vol. 23, p. 101654, 2021, doi: 10.1016/J.ETI.2021.101654.

[15] Y. Wang *et al.*, "Selenium Nanoparticle Synthesized by Proteus mirabilis YC801: An Efficacious Pathway for Selenite Biotransformation and Detoxification," *Int J Mol Sci*, vol. 19, p., 2018, doi: 10.3390/ijms19123809.

[16] V. A. Schommer *et al.*, "Biochar-immobilized Bacillus spp. for heavy metals bioremediation: A review on immobilization techniques, bioremediation mechanisms and effects on soil.," *Sci Total Environ*, p. 163385, 2023, doi: 10.1016/j.scitotenv.2023.163385.

[17] Z. Moussa, D. Darwish, S. Alrdahe, and W. Saber, "Innovative Artificial-Intelligence- Based Approach for the Biodegradation of Feather Keratin by Bacillus paramycoides, and Cytotoxicity of the Resulting Amino Acids," *Front Microbiol*, vol. 12, p., 2021, doi: 10.3389/fmicb.2021.731262.

[18] A. Rashid, S. Mirza, C. Keating, S. Ali, and L. Campos, "Indigenous Bacillus paramycoides and Alcaligenes faecalis: potential solution for the bioremediation of wastewaters," *bioRxiv*, p., 2020, doi: 10.1101/2020.05.20.105940.

[19] X. Chen, H. Lin, Y.-B. Dong, B. Li, C. Liu, and T. Yin, "Mechanisms underlying enhanced bioremediation of sulfamethoxazole and zinc(II) by Bacillus sp. SDB4 immobilized on biochar," *J Clean Prod*, p., 2022, doi: 10.1016/j.jclepro.2022.133483.

[20] S. Borah *et al.*, "Selenite bioreduction and biosynthesis of selenium nanoparticles by Bacillus paramycoides SP3 isolated from coal mine overburden leachate.," *Environmental pollution*, vol. 285, p. 117519, 2021, doi: 10.1016/J.ENVPOL.2021.117519.

[21] T. Disz *et al.*, "Accessing the SEED Genome Databases via Web Services API: Tools for Programmers," *BMC Bioinformatics*, vol. 11, p. 319, 2010, doi: 10.1186/1471-2105-11-319.

[22] K. Keegan, E. Glass, and F. Meyer, "MG-RAST, a Metagenomics Service for Analysis of Microbial Community Structure and Function.," *Methods in molecular biology*, vol. 1399, pp. 207–233, 2016, doi: 10.1007/978-1-4939-3369-3_13.

[23] T. Brettin *et al.*, "RASTtk: A modular and extensible implementation of the RAST algorithm for building custom annotation pipelines and annotating batches of genomes," *Sci Rep*, vol. 5, p., 2015, doi: 10.1038/srep08365.

[24] R. Aziz *et al.*, "The RAST Server: Rapid Annotations using Subsystems Technology," *BMC Genomics*, vol. 9, p. 75, 2008, doi: 10.1186/1471-2164-9-75.

[25] R. Overbeek *et al.*, "The SEED and the Rapid Annotation of microbial genomes using Subsystems Technology (RAST)," *Nucleic Acids Res*, vol. 42, p., 2013, doi: 10.1093/nar/gkt1226.

[26] C. Söhngen, B. Bunk, A. Podstawka, D. Gleim, and J. Overmann, "BacDive—the Bacterial Diversity Metadatabase," *Nucleic Acids Res*, vol. 42, p., 2013, doi: 10.1093/nar/gkt1058.

[27] I. Schober *et al.*, "BacDive in 2025: the core database for prokaryotic strain data," *Nucleic Acids Res*, vol. 53, p., 2024, doi: 10.1093/nar/gkae959.

[28] R. Olson *et al.*, "Introducing the Bacterial and Viral Bioinformatics Resource Center (BV-BRC): a resource combining PATRIC, IRD and ViPR," *Nucleic Acids Res*, p., 2022, doi: 10.1093/nar/gkac1003.

[29] C. Söhngen *et al.*, "BacDive – The Bacterial Diversity Metadatabase in 2016," *Nucleic Acids Res*, vol. 44, p., 2015, doi: 10.1093/nar/gkv983.

[30] L. Reimer, J. Carbasse, J. Koblitz, C. Ebeling, A. Podstawka, and J. Overmann, "BacDive in 2022: the knowledge base for standardized bacterial and archaeal data," *Nucleic Acids Res*, vol. 50, p., 2021, doi: 10.1093/nar/gkab961.

[31] K. Aoki and M. Kanehisa, "Using the KEGG Database Resource," *Curr Protoc Bioinformatics*, vol. 11, p., 2005, doi: 10.1002/0471250953.bi0112s11.

[32] M. Kanehisa, M. Furumichi, M. Tanabe, Y. Sato, and K. Morishima, "KEGG: new perspectives on genomes, pathways, diseases and drugs," *Nucleic Acids Res*, vol. 45, p., 2016, doi: 10.1093/nar/gkw1092.

[33] M. Kanehisa, Y. Sato, M. Kawashima, M. Furumichi, and M. Tanabe, "KEGG as a reference resource for gene and protein annotation," *Nucleic Acids Res*, vol. 44, p., 2015, doi: 10.1093/nar/gkv1070.

[34] R. Adamczak, A. Porollo, and J. Meller, "Combining prediction of secondary structure and solvent accessibility in proteins," *Proteins: Structure*, vol. 59, p., 2005, doi: 10.1002/prot.20441.

[35] T. Petersen *et al.*, "Prediction of protein secondary structure at 80% accuracy," *Proteins: Structure*, vol. 41, p., 2000, doi: 10.1002/1097-0134(20001001)41:1<17::AID-PROT40>3.0.CO;2-F.

[36] C. Geourjon and G. Deléage, "SOPMA: significant improvements in protein secondary structure prediction by consensus prediction from multiple alignments," *Comput Appl Biosci*, vol. 11 6, pp. 681–684, 1995, doi: 10.1093/bioinformatics/11.6.681.

[37] N. Guex and M. Peitsch, "SWISS-MODEL and the Swiss-Pdb Viewer: An environment for comparative protein modeling," *Electrophoresis*, vol. 18, p., 1997, doi: 10.1002/elps.1150181505.

[38] N. Guex, M. Peitsch, and T. Schwede, "Automated comparative protein structure modeling with SWISS-MODEL and Swiss-PdbViewer: A historical perspective," *Electrophoresis*, vol. 30, p., 2009, doi: 10.1002/elps.200900140.